Molecular Crystals and Liquid Crystals Science and Technology. Section A. Molecular Crystals and Liquid Crystals

Publication details, including instructions for authors and subscription information:
http://www.tandfonline.com/loi/gmcl19

Physical Features of Low Dimensional Organic Super-conductors

J. P. Pouget [a]

[a] Laboratoire de Physique des Solides (CNRS URA 2) Bailment 510, Université Paris-Sud, 91405, ORSAY, France

Version of record first published: 24 Sep 2006.

To cite this article: J. P. Pouget (1993): Physical Features of Low Dimensional Organic Super-conductors, Molecular Crystals and Liquid Crystals Science and Technology. Section A. Molecular Crystals and Liquid Crystals, 230:1, 101-131

To link to this article: http://dx.doi.org/10.1080/10587259308032220

Mol. Cryst. Liq. Cryst. 1993, Vol. 230, pp. 101–131
Reprints available directly from the publisher
Photocopying permitted by license only

Printed in the United States of America

PHYSICAL FEATURES OF LOW DIMENSIONAL ORGANIC SUPERCONDUCTORS

J.P. POUGET
Laboratoire de Physique des Solides (CNRS URA 2)
Bâtiment 510, Université Paris-Sud, 91405 ORSAY (France)

Abstract Since the discovery of the organic superconductivity more than 10 years ago with a critical temperature (T_S) of 1 K in quasi one dimensional (1D) conductors based on the tetramethyltetraselenafulvalene molecule, more than 40 organic superconductors are now known, achieving T_S up to about 13 K. These salts are made of π quasi-planar donors or acceptors, orbitals of which overlap very anisotropically. As a consequence of the 1D or 2D anisotropy of the electron gas, the superconducting ground state competes with charge or spin density wave ground states and the electronic properties are strongly influenced by the occurrence of order-disorder transitions involving molecular orientational or conformational degrees of freedom. In this framework we review the present understanding of the physical properties of the main families of low dimensional organic superconductors and we compare their physical features with those shown by the family of 3D fullerenes exhibiting T_S higher than 30 K.

I. HISTORICAL INTRODUCTION

For a long time organic materials were know only as semiconductors or as insulators.Metallic properties were recognized and extensively studied in the 70' s with the discovery of several families of charge transfer salts based on the tetracyanoquinodimethane (TCNQ) donor and on the tetrathiafulvalene (TTF) acceptor. Charge transfer salts are composed of segregated stacks of donors (D) and acceptors (A). The metallic character of both kinds of stack is due to a partial charge transfer from D to A ($\rho = 0.59$ in TTF-TCNQ). With a good Pπ molecular orbital overlap in the stacking direction and a poor overlap between stacks, one dimensional (1D) metallic properties are observed at room temperature. However the metallic properties of these materials cannot be maintained down to low temperature because of the occurrence of a Peierls metal-insulator phase transition at about $T_p \sim 50$ K[1]. It is driven by the instability of the 1D electron gas towards the formation of charge density waves (CDW) of wave vector $2k_F$ ($= \rho \pi / a$, if a is the stacking periodicity) where the electronic density is modulated in chain direction via an intrastack displacement of the molecules.

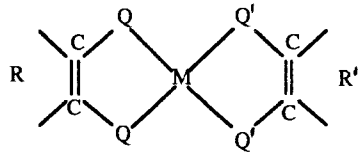

Table I : Donor (D) and acceptor (A) molecules, anions (X) and cations (Y) giving rise to organic supraconductors. The critical temperature of superconductivy (T_S) and the electronic dimensionality are also indicated

M	Q, Q'	R, R'	molecule	Electronic dimensionality	T_s	X in D_2X
C = C	Q = Q' = Se	R = R' : CH_3, CH_3	TMTSF	quasi-1D	1.2 K	PF_6,ClO_4,ReO_4,--
	Q = Q' = S	Q" = S : R = R' : Q", CH_2, CH_2, Q"	BEDT-TTF	quasi-1D (?)	2 K	ReO_4
				2D(β phase)	1.4-8.1 K	I_3, AuI_2,IBr_2
				2D (κ phase)	3.6 - 12.8 K	I_3,$Cu(NCS)_2$,$Cu[N(CN)_2]L$ (L = Cl,Br,CN)
		Q" = O :	BEDOTTF	2D (?)	~ 1 K	ReO_4 (+H_2O)
	Q = Se Q' = S	R of TMTSF R' of BEDT-TTF	DMET	quasi-1D	0.6-0.9 K	I_3, IBr_2, AuL_2,(L=Cl,Br,I,CN)
				2D (κ-phase)	1.9 K	Au Br_2
	Q = Q' = S	R : H, H ; R' : S, CH_2, S	MDT-TTF	2D (κ-phase)	4.5 K	Au I_2
						Y in Y A_2
Ni, Pd	Q = Q' = S	R = R' : S, C = S, S	M(dmit)$_2$	quasi-1D	1.6 K (Ni) 6.5 K (Pd)	TTF 〃
				quasi-1D	5 K (Ni) 6.2 K (Pd)	$(CH_3)_4N$ 〃

A real breakthrough occured in 1979 with the stabilization of the metallic state under pressure and the discovery of organic superconductivity at $T_S \sim 1$ K in$(TMTSF)_2 PF_6$, which is based on the tetramethyltetraselenafulvalene donor [2]. With different monovalent anions X such as PF_6,ClO_4, ReO_4,... a whole family of quasi-1D conductors, now known as the $(TMTSF)_2X$ Bechgaard salts,and which present an impressive number of novel physical features and new electronic ground states, were synthesised [3a,4].

The second important donor molecule leading to a sizeable increase of T_S was the TTF derivative bis (ethylenedithio)tetrathiafulvalene, BEDT-TTF or simply ET . With anions X such I_3,$Cu(NCS)_2$,... $(ET)_2X$ quasi-2D organic conductors were obtained with critical superconducting temperatures, approching and even overcoming the "10 K barrier" [3b,4].

Up to now more than 40 organic superconductors have been reported belonging to the main families of organic molecules shown Table I. Nearly all of the superconductors are D_2X salts based on donors . Two noticeable exceptions are the quasi 1-D YA_2 salts based on the metal-organic acceptor complexes $M(dmit)_2$ and the recently discovered 3D fullerene materials Y_3C_{60}[3c], exhibiting the highest critical temperatures, with a T_S ranging from 19 K (Y = K) to 33 K ($Y_3 = Cs_2Rb$).

In this paper we shall present, following a recent review of organic conductors [5], a comparative survey of these organic superconductors with a special emphasis to physical parameters such as the dimensionality of the electron gas, the electron-electron interactions and the coupling between electronic and structural degrees of freedom which control their properties.

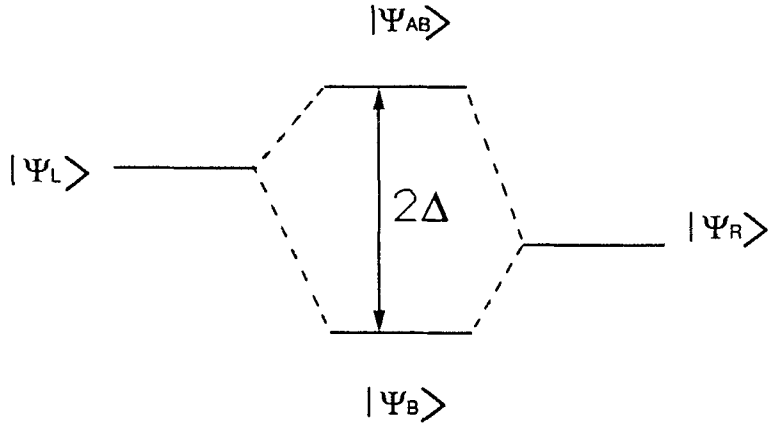

Figure 1
Simple description of the HOMO-LUMO splitting using bonding and antibonding combinations of orbitals constructed on left and right molecular moities.

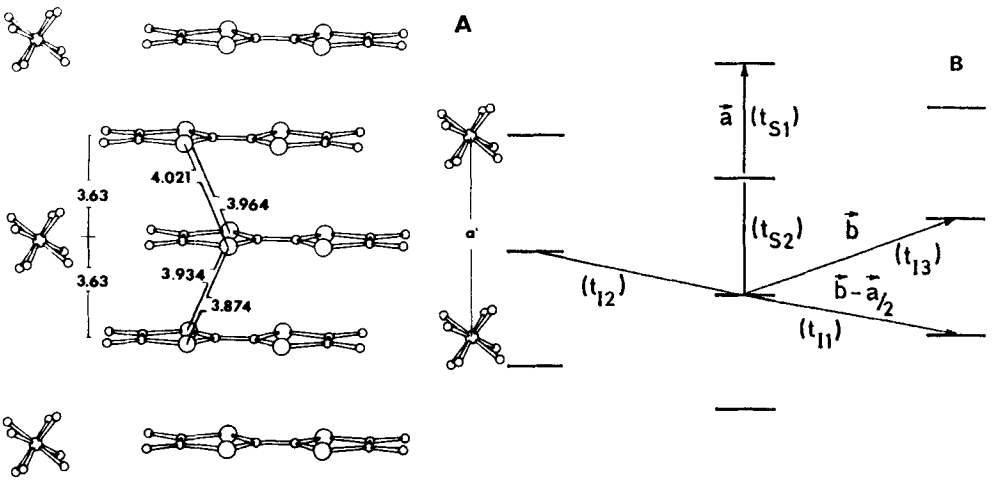

Figure 2
a) Side view $(TMTSF)_2X$ showing the stack of donors,
b) (a,b) array of donors in $(TMTSF)_2X$. The most important transfer integrals are indicated.

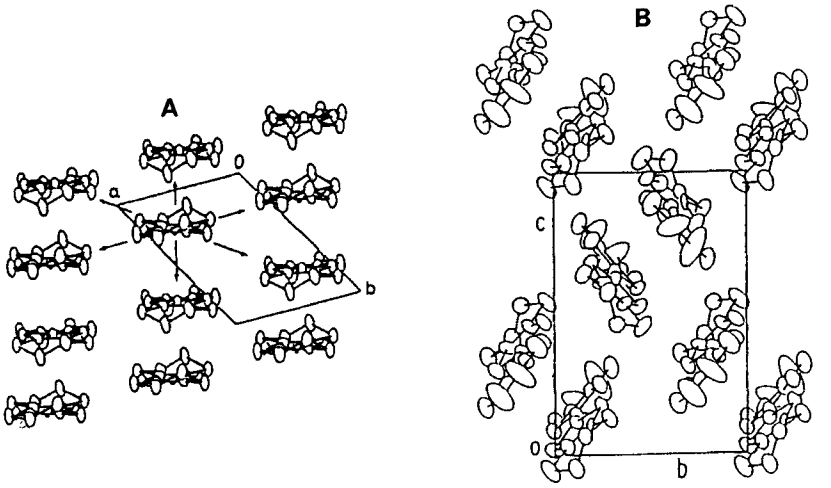

Figure 3
a) Stacking arrangement of ET molecules in the (a,b) plane of $\beta(ET)_2 I_3$ viewed from the long molecular axis.
b) Arrangement of dimers of ET molecules, viewed from the a axis of κ-$(ET)_2Cu(NCS)_2$.

II. ELECTRONIC STRUCTURE

The conduction band of charge transfer salts is generally built from the highest occupied molecular orbital (HOMO) of donors or the lowest unoccupied molecular orbital (LUMO) of acceptors. With the molecules despicted in Table I these orbitals can be obtained from bonding and antibonding combinations of orbitals built on the left and right molecular moities (Fig.1). The splitting 2Δ depends on the overlap of these $P\pi$ orbitals through the bridging entity M. For the donors shown Table I, there is a large overlap though the C = C double bond. Thus with $\Delta \sim 1.5$ eV, larger than the intermolecular transfer integral $t_a \sim 0.25$ eV, only the HOMO are relevant to describe the conduction band of these donors. Such is not the case for the $M(dmit)_2$ acceptor for which there is a weak overlap through the Ni or Pd transition metal. Thus with $\Delta \sim 0.2$ eV comparable to t_a, both the HOMO and LUMO must be considered for a correct description of the conduction band structure [6]. Several orbitals (t_{1u} 3-fold degenerate LUMO of the C_{60}) are also required to describe the C_{60}^{3-} band structure of the $(Alkaline)_3$ C_{60} superconducting materials [7].

Radical-cation-based organic superconductors are layered materials where sheets of donors alternate with sheets of inorganic anions, as shown figure 2a for the case of $(TMTSF)_2X$. Figure 2b presents a schematic arrangement of the TMTSF molecules in the (a,b) layer. TMTSF molecules form slightly dimerized stacks along the a (1D) direction. There is also a noticeable interstack overlap between P_π orbitals, whose sign and magnitude depend critically on the relative disposition of neighbouring stacks [13] : a key factor to control the dimensionality of the electron gas. Figure 3 presents the molecular arrangement of the ET based conductors $\beta(ET)_2I_3$ (a) and $\kappa(ET)_2$ $Cu(NCS)_2$ (b).The ET network of the β phase is analogous to that of the TMTSF salts : ET molecules form dimerized linear stacks along $\vec{a} + \vec{b}$ .The κ phase is composed of face to face ET dimers, which are oriented approximately at right angles with respect to their neighbors, forming a 2D conducting network.

It is important to point out that the crystal packing is governed by cohesion forces involving the σ molecular orbitals (Se..Se intermolecular contacts , Se.. anion and CH_3... anion contacts in $(TMTSF)_2X$; C-H.. donor and C-H.. anion contacts involving the ethylene groups in $(ET)_2X$). The minor role played by the π conduction orbitals in the cohesion energy is well illustrated in $(TMTSF)_2X$ by the observation that the TMTSF stacks are dimerized in such a way that the intradimer

distances are close to the anions X, a feature which does not minimize the Coulomb forces between the anions and the π electrons. This structural remark allows to understand that the decrease of dimerization, observed upon cooling in the S analogues $(TMTTF)_2X$ [8], corresponds to a reduction of the π electron-anion Coulomb repulsion terms. Finally let us remark that any structural modifications changing the σ electronic distribution will also influence the π electronic cloud through intramolecular electron (σ) - electron (π) correlations.

The basic features of the intralayer HOMO band dispersion of these salts can be simply understood using the tight binding band dispersion of a rectangular lattice with one molecule (Z = 1) per unit cell (fig.4a):

$$E(k) = 2t_a \cos h\, a' + 2t_\perp \cos k\, d_\perp \qquad (1)$$

where, with respect to fig. 2b, the stack dimerization has been neglected ($t_a \sim t_{s1} \sim t_{s2}$) and where $t_\perp$ mimics a complex combination of the $t_{\perp i}$ [4]. The conduction band structure of the $(TMTSF)_2X$, with a unit cell of Z=2 molecules along a (fig.2), is obtained by folding the band dispersion (1) across XS (fig.4b). The degeneracy on the zone boundary along XS is suppressed by the dimerization of the stacks [9]. The band structure of $\beta(ET)_2X$, with a unit cell of 2 molecules along $\vec{a} + \vec{b}$ (fig. 3a), is obtained by folding the band dispersion (1) across X'Y' (fig.4c). In $\beta(ET)_2X$ the 2 conduction bands are no longer degenerate at the zone boundary X'Y' because of the dimerization of the ET network[10]. Because of the transverse doubling of the periodicity, the band structure of $(ET)_2ReO_4$ (Z = 4) is obtained by folding that of $(TMTSF)_2X$ across MY (fig. 4d). The stack dimerization as well as the "$+d_\perp$","$-d_\perp$" asymmetry the $t_{\perp i}$'s lift the degeneracies at the X,M,Y points [11]. $\kappa(ET)_2X$ salts are composed of 2 dimers per unit cell (fig.3b). The intradimer overlap integral is stronger than the interdimer one [12b]. Thus the band structure can be viewed as the dispersion of the bonding and antibonding levels of each dimer. The dispersion of each level is basically that shown Fig. 4c, with an interdimer overlap $t_{eff} \sim 2t_a \sim 2t_\perp$ [12a].

Because of the 2 : 1 stoichiometry and of the complete charge transfer to the anion, each cation HOMO is 3/4 filled. Fig.5a and b show the Fermi surfaces (FS) of $(TMTSF)_2PF_6$ [9c] and β $(ET)_2I_3$ [10c] respectively in the (a*, b*) reciprocal plane. Only one conduction band cuts the Fermi level and with Z = 2 molecules per unit cell the 2D Brillouin zone is half filled. The opening or closing of the FS depends upon

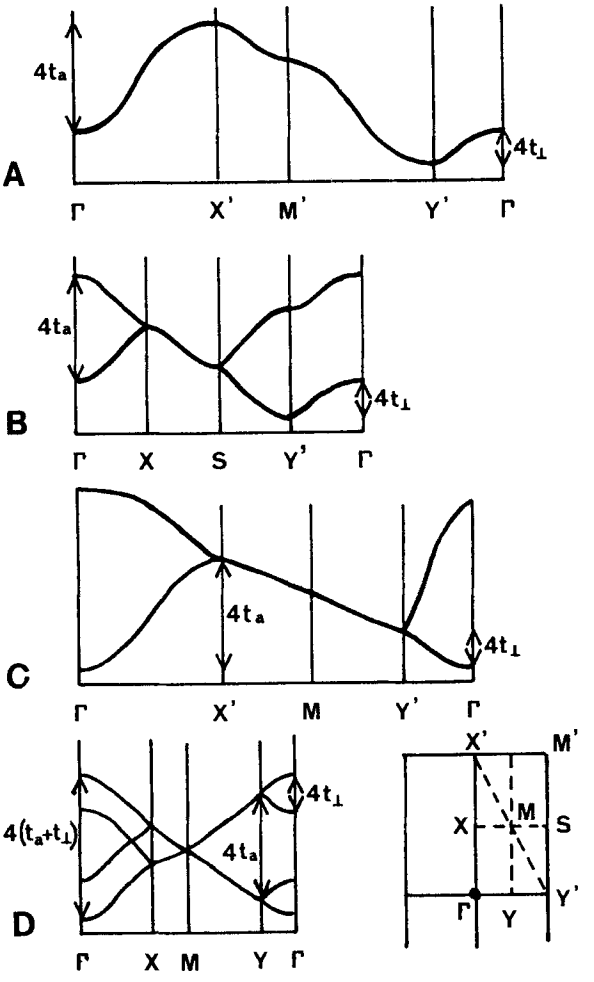

Figure 4
Band dispersions given by equation (1) in :
a) the "ΥX' M'Y' " Brillouin zone ,
(b) the 2-fold "ΥXSY'" Brillouin zone,
(c) the 2-fold "ΥX'M Y'" Brillouin zone,
(d) the 4-fold "ΥXMY" Brillouin zone.
In (a) and (b) $t_\perp$ is > 0 (case of $(TMTSF)_2X$), in (c) $t_\perp < 0$ (case of $(ET)_2X$) . t_a is < 0.

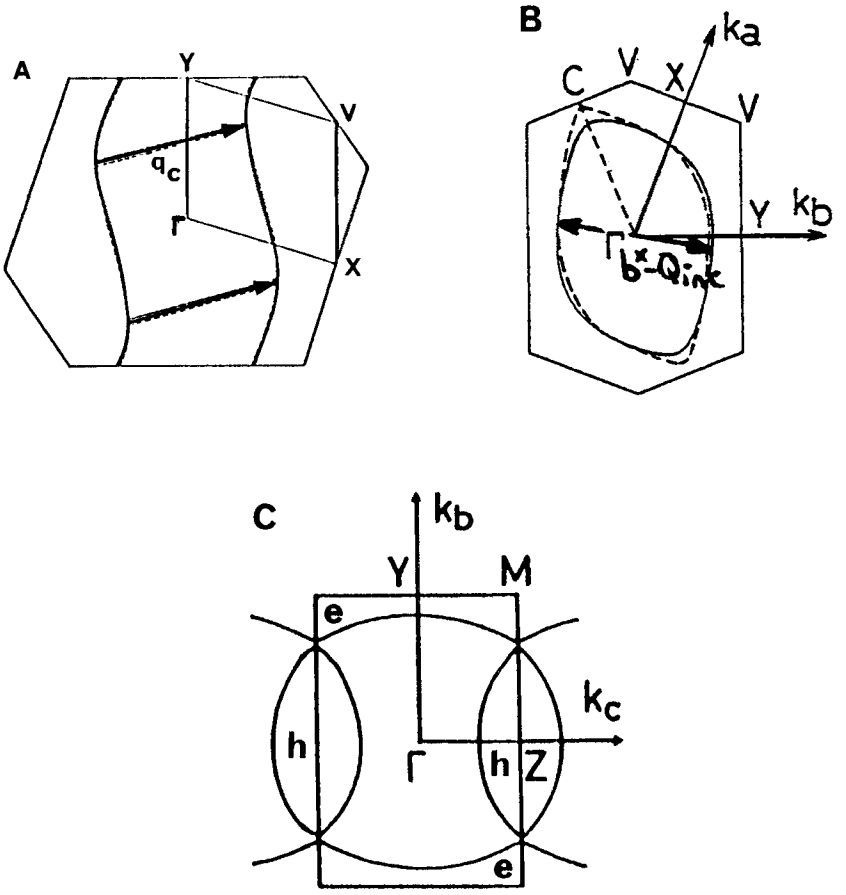

Figure 5

Fermi surfaces of : a) $(TMTSF)_2PF_6$ at 4 K. The best nesting wave vector $\vec{q_c}$ is indicated (from ref. 9c) ; b) $\beta(ET)_2I_3$, with transfer integrals adjusted on the thermopower data (from ref. 10c). The nesting wave vector $\vec{b^*} - \vec{Q_{inc}}$ discussed in the text is shown ; c) $\kappa(ET)_2Cu(NCS)_2$.h and e denote hole and electron pockets respectively.

the relative magnitude of t_a and $t_\perp$. Fig. 5c shows the FS of $\kappa(ET)_2 Cu(SCN)_2$[12]. Two conduction bands cut the Fermi level. They achieve metallic conduction, because otherwise with Z = 4 molecules per unit cell all the occupied states of one conduction band will fill the 2D Brillouin zone.

The F.S. of $(TMTSF)_2X$ is warped but open (fig. 5a). The quasi-1D anisotropy of these salts is proved by optical polarized reflectance [14] which analysis gives t_a ~ 0.25 eV and $t_\perp$ ~ 22 meV.The open FS is due to the large anisotropy of transfer integrals : $t_a/t_\perp$ ~ 10. Such a ratio agrees with the measured intralayer anisotropy of conductivity of 25-200 (see table II) :

$$\frac{\sigma_a}{\sigma_\perp} \sim \left(\frac{t_a}{t_\perp}\ \frac{a'}{d_\perp}\right)^2 \qquad (2)$$

where $d_\perp$ ~ 1.8 a', In (2) an interchain diffusive movement of carriers is assumed. $(ET)_2ReO_4$ is close to the critical ratio $t_a/ t_\perp$ for which a cross over from open to close F.S. occurs when there is Z = 2 formula per unit cell. Band calculations give a closed FS with a ratio $t_a/ t_\perp$ ~ 2-3 [11], about 3 times smaller than the ratio deduced from the measured intralayer conductivity anisotropy of 20. With this last value and knowing that with a smaller ratio of anisotropy the FS of $\beta(ET)_2 I_3$ is nearly opened (fig. 5b), an open FS is expected for $(ET)_2 ReO_4$ in an extended Brillouin zone description corresponding to Z = 2.

$\beta(ET)_2 X$ (X = I_3, I Br_2) has a closed F.S. in the layer of donor molecules (Fig. 5b), in agreement with the observation of giant magnetoresistance (Shubnikov de Hass, SdH) oscillations when the magnetic field is applied along the interlayer direction, and which main frequency corresponds, as expected for Z = 2, to about one carrier per unit cell [15]. The shape of the FS of the IBr_2 salt has been reconstructed from angular magnetoresistance oscillations [16]. Its transverse cross section resembles quite well that of the I_3 salt obtained from tight binding band calculations with parameters adjusted to fit the thermopower data (fig. 5b) [10c]. Intralayer reflectance mesuarements [17] lead, from the plasma frequencies (ω_p), to an effective mass anisotropy :

$$\frac{m_2^*}{m_1^*} = \frac{t_1 d_1^2}{t_2 d_2^2} = \frac{\sigma_1}{\sigma_2} = \frac{\omega p_1^2}{\omega p_2^2} \qquad (3)$$

of 3.5 is good agreement with the reported intralayer conductivity anisotropy of 2.5 (table II). With $d_1 \sim d_2$, relationship (3) gives a similar value for the anisotropy ratio of the intrastack and interstack transfer integrals. It means that the FS of $\beta(ET)_2I_3$ is not too far to be opened in the ΥC direction, the perpendicular at the $\vec{a} + \vec{b}$ stacking direction (see fig. 5b).

The intralayer FS of $\kappa(ET)_2$ Cu $(NCS)_2$, shown fig.5c, resembles that calculated for $(ET)_2ReO_4$ [11]. It is closed, but it intersects the zone boundary in the ΓZdirection. Its topology has been accurately verified by SdH magnetoresistance [18] and (de Haas-van-Halphen dHvH)[22] magnetization oscillations. It is constituted of two parts :

(i) - a lens-hole-like closed FS, centered at the Z point and corresponding to ~ 18% of the surface of the 2D Brillouin zone,

(ii) a quasi-1D electron like open FS, parallel to the Y-M line.

The associated two conduction bands are separated by an energy gap of ~ 60 K along the Z-M line. The F.S (i) is responsible of the positive sign of the thermoelectric power in the c direction and the F.S (ii) is responsible of its negative sign in the b direction [10c,19]. The effective mass anisotropy deduced from reflectivity data eq.(3), is of about 1.5[17b], in fair agreement with the intralayer conductivity anisotropy of ~ 2 (table II).

	σ_a (S/cm)	$\left.\frac{\sigma_a}{\sigma_\perp}\right\|_{intra}$	$\left.\frac{\sigma_a}{\sigma_\perp}\right\|_{inter}$
$(TMTSF)_2X$	400 - 800	25 (ClO_4) 200 (PF_6)	900 (ClO_4) 3.10^4 (PF_6)
$(ET)_2 ReO_4$	200	20	?
$\beta(ET)_2 I_3$	30	2.5	600
κ-$(ET)_2Cu(NCS)_2$	30	2	$1.5\ 10^3$

Table II

Highest conductivity σ_a, intraplanar and interplanar anisotropies at room temperature of some quasi-1D and 2D organic conductors

The F.S. of all these salts is opened in the interlayer direction, but warped due to the finite value of the interplane transfer integral (t_{inter}). The topology of the corrugated FS gives rise to fine structure or peaks in the angular dependence of the magnetoresistance of quasi-1D conductors,such as $(TMTSF)_2X$ [20], or 2D conductors, such as the $(ET)_2X$ salts [21], respectively. The warping of a 2D cylindrical FS gives rise to a beating pattern in the SdH or dHvH oscillations, allowing to estimate an anisotropy ratio of transfer integrals, $t_{intra}/t_{inter} \sim 10^2$, in fair agreement with that deduced from the anisotropy of conductivity (Table II), using the relationship (2) with $d_{inter} \sim 2.5\, d_{intra}$. This leads, with $t_{intra} \sim 0.1$ eV estimated from plasma frequency measurements [17a] to $t_{inter} \sim 1$ meV. The conductivity anisotropy in the $(TMTSF)_2X$ series gives similar values of t_{inter}.

Finally let us remark that if the FS approaches the Brillouin zone boundaries, as in the β phases near the C point, its warping, due to t_{inter}, can lead to intersections with these boundaries. This will form necks joining neighbouring FS cylinders in a extended zone schema, leading to unusual features in the angular magnetoresistance dependence. Such effects seem to have been detected in β $(ET)_2IBr_2$ [16]. They does not occur in κ$(ET)_2Cu(NCS)_2$,where dHvH studies [22] show that the cylindrical F.S. is only weakly corrugated.

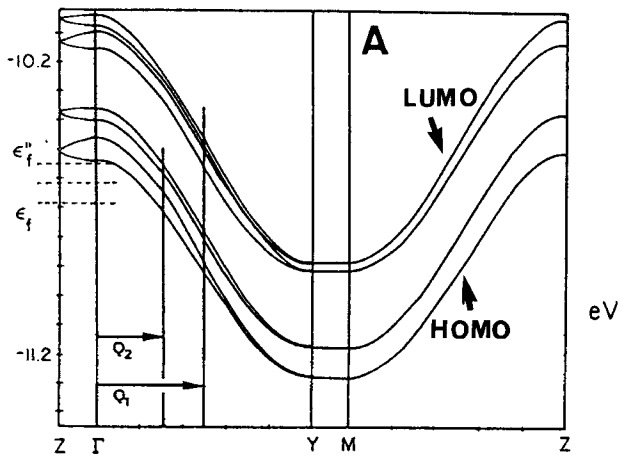

Figure 6
Band structure of $Pd(dmit)_2$ slabs in $TTF[Pd(dmit)_2]_2$ (from ref. 23).

Half the 1D critical wave vectors $2k_F$ measured by X-ray diffuse scattering (ref.41) are indicated.

The acceptor based conductors $Y[M(dmit)_2]_2$, M = Ni, Pd, are quasi-1D conductors. Band calculations lead, with lattice parameters determined at ambiant conditions, to open FS [23]. However in some of the salts, the FS is so significantly warped that minor parameter contractions, as this usually occurs under pressure, could easily close the FS. The unusual features exhibited by the Y = TTF salts is that both the bands derived from the HOMO and LUMO of the $M(dmit)_2$ cut the Fermi level, as shown on figure 6.

Y_3C_{60} (Y = K,Rb) superconducting materials adopt the faced centered cubic system which FS has not been experimentally determined. However thermopower measurements (S) show that electrons are the dominant carriers. Assuming an isotropic FS, the linear dependence of S with T gives a Fermi energy (E_F) ~ 0.2 (Rb)-0.3(K) eV or an effective mass 5 - 3.5 m_e comparable to that found in others organic superconductors [24].

III. ELECTRON-ELECTRON AND ELECTRON-PHONON INTERACTIONS

These interactions have been neglected in section II devoted to a one electron description of the average structure. A special feature of organic solids composed of molecules which size is comparable with the intermolecular spacing is that the intramolecular Coulomb repulsion (U) is of the same magnitude of the 1st neighbor intermolecular Coulomb repulsion term (V_1). The importance of electron-electron interactions was demonstrated in the TTF-TCNQ family of 1D organic charge transfer salts from a carrefull analysis of optical absorption spectra [25] and NMR T_1 relaxation rate measurements [26]. Its main consequence is the formation of $4k_F$ CDW where, via the electron-phonon coupling, the localization of charge with an average periodicity of $a/\rho = 2\pi/4k_F$ leads to a concomitant lattice distortion which has been observed by X-ray diffuse scattering experiments [27]. In TTF-TCNQ it is estimated that $U/4t_a$ ~ 1-3 and U/V_1 ~ 2-3 [5]. The actual values of these parameters for other salts however depend on the molecular species (U decreases when the size and polarizability of the molecules increase, which occurs along the sequence TTF, TMTTF, TMTSF, BEDT-TTF) and on the molecular arrangement (t_a is a very sensitive function of the overlap between molecular orbitals).

An intermediate coupling regime of electron-electron interactions can be inferred from the analysis of NMR data [28] and infrared oscillator strength measurements [29] in the quasi-1D $(TMTSF)_2X$ series. Coulomb interactions are enhanced in the S analogue $(TMTTF)_2X$ series, as shown by the observation of charge localization phenomena on transport properties below about 200 K [30], and NMR evidences of

important 1D quantum antiferromagnetic (i.e. $2k_F$) fluctuations up to room temperature [28]. The charge localization, which increases with the strength of the anion-donor interactions along the sequence PF_6, AsF_6, SbF_6 [30b], is believed to be caused by the $4k_F$ CDW response of organic stack, which also increases from TMTSF to TMTTF, to the $4k_F$ potential of the anion sublattice [31]. Similar localization phenomena are observed in others series of TTF based donors, such as $(t\text{-TTF})_2X$, $(BCP\text{-TTF})_2X$ and $(DIMET)_2X$, and S/S_e mixed donors, such as $(TMDTDSF)_2X$ and $(DMET)_2X$, which stacks are weakly dimerized as in the Bechgaard salts (i.e. type I salts of ref. 32). A strongest electronic localization is observed in type II salts such as $(ET)_2X$ with $X = ICl_2$ and $AuCl_2$, when the donor layer is constituted of weakly interacting dimers.

The important role of the electron-electron interactions in the physical properties of these organic salts will become more evident in the next section with the report of antiferromagnetic and spin Peierls ground states. In a similar way the recent report of a magnetic ground state ($T_c \sim 16$ K) in (TDAE) C_{60} [33] points out the relevance of Coulomb interactions in fullerene materials.

Important phenomena are also associated with the coupling between electronic and structural degrees of freedom. As usual in molecular crystals there are two important sources of electron-phonon coupling :

- coupling with external modes. This coupling, which modulates the transfer integral t_a, is responsible of the $2k_F$ and $4k_f$ CDW instabilities observed in the phonon acoustic branches of charge transfer salts. The associated dimensionless electron-(acoustic) phonon interaction can be estimated at about $\lambda_{ac} \sim 0.2$ from the analysis of the X-ray diffuse scattering data of TSF-TCNQ [34].

- coupling with internal modes (electron molecular vibration, EMV, coupling). It modulates the HOMO or LUMO energy levels. For a non degenerate level only the totally symmetric Ag vibration modes couple linearly to the conduction electrons which intermolecular oscillations or movements induce spectacular features in the infrared (IR). Two important coupling with the HOMO occurs via the C-S and C=C stretching modes of the TTF molecule for which it is estimated dimensionless EMV constants, λ_{opt}, of about 0.3 and 0.2 respectively [4]. These EMV induced IR modes have been detected in many TTF, TMTTF, TMTSF and ET salts. Dynamical charge transfers induced by the Ag vibration modes have also been observed by Raman scattering in $(TMTSF)_2X$ materials [35].

There is also an important coupling between the π electronic cloud and the orientational (case of non centrosymmetrical anions X or cations Y located in a

symmetrical cavity) or conformational (case of the ethylene groups of the ET molecule) degrees of freedom of the various molecular entities. Consequences on the electronic properties of such a coupling will be discussed in section V.

Until now we have mainly discussed the electron-electron and electron-phonon interactions in quasi-1D conductors. Their importance in 2D ET-based conductors and superconductors is still debated. For example the semiconductor to metal crossover observed upon cooling in various κ salts (table IV) has been interpreted a being the signature either of important Mott Hubbard electron correlations [36] or of important electron-phonon coupling leading to the formation of small polarons [37]. We shall propose in Section V that this electron localization - delocalization phenomena could be related to a conformational disorder-order transition of the ethylene groups of the ET molecule. The same debate concerns the origine of the large effective mass ($m \sim 4\ m_e$) measured by SdH and dHvA studies of the 2D ET salts. On one hand electron-electron interactions were claimed to be important in $(ET)_2KHg(SCN)_4$ from the determination of a SdH transport mass 3-5 times more important than the band effective mass measured by FIR cyclotron resonance or plasmon frequencies [38]. On the other hand the slight mass enhancement determined from the same set of dHvA data in $\alpha(ET)_2(NH_4)Hg(SCN)_4$ and κ-$(ET)_2Cu(NCS)_2$ was interpreted as due to the electron-phonon coupling with a dimensionless coupling constant $\lambda \sim 0.5$ [22].

IV. PHASE DIAGRAMS

Organic conductors exhibit complex phase diagrams where the superconductor ground state either competes with charge (CDW) or spin density waves (SDW) insulating ground states or is strongly dependent upon subtle structural modifications. Their understanding requires to go beyond the one electron description and to consider the influence of electron-electron and electron-phonon interactions.

Let us begin with quasi-1D conductors. Depending on the range and on the strength of Coulomb repulsions, a purely 1D gas exhibits instabilities towards either $2k_F$ SDW or $2k_F$ (and/or $4k_F$) CDW or singlet or triplet superconductivity (the $2k_F$ wave vector nests the Fermi level states of a 1D band which is filled from $-k_F$ to $+k_F$). At high temperature all these channels interfere. The interferences are suppressed by the interchain coupling (i.e. below $k_BT \sim \tilde{t}_\perp/\pi$) and the ground state stabilized depends upon the nature and the strength of the 1D response function and of the interchain coupling.

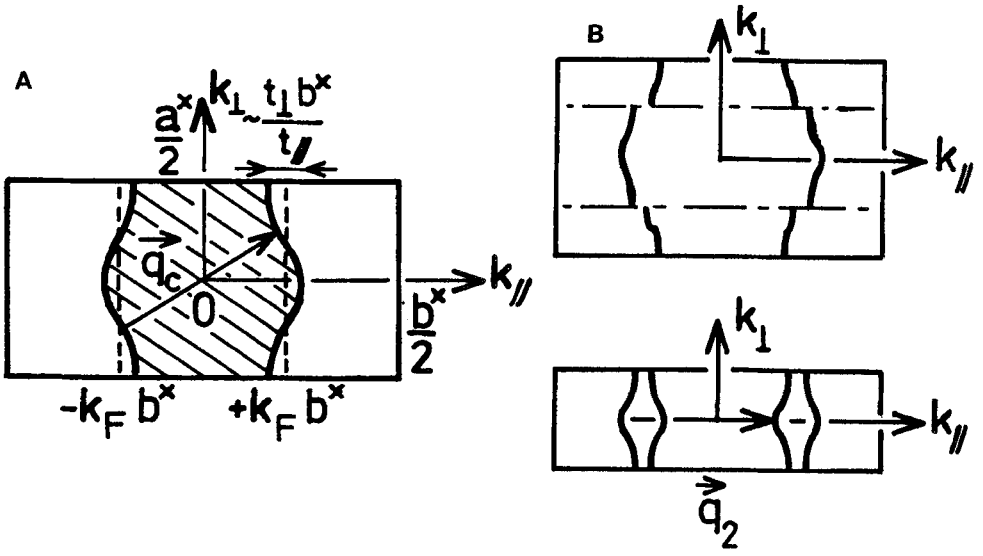

Figure 7

a) Warped open Fermi surface and its nesting wave vector $\vec{q}_c$,

b) Tranversally folded Fermi surface and its $\vec{q}_2 = (\frac{1}{2},0)$ wave vector of nesting

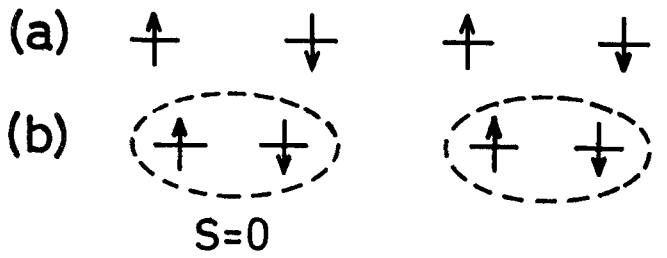

Figure 8
Schematic representation of the antiferromagnetic (a) and spin-Peierls (b) groundstates.

In the weak coupling limit, the density wave transition corresponds to a metal-insulator transition and the resulting gain of electronic energy selects the best nesting wave vector of the FS (i.e. the one which connects its inflection points, Fig. 7a). The SDW ground state is observed in $(TMTSF)_2PF_6$ below a 2nd order phase transition at T_{SDW} = 12 K (at Patm).The wave vector of modulation determined by proton NMR [39], $\vec{Q_c} = 0.5\vec{a}^* + 0.2\vec{b}^*$, nests relatively well the calculated open FS (fig. 5a). A CDW ground state is observed below a 1st order phase transition at 77 K in $(ET)_2ReO_4$ [20]. The first two components of the CDW wave vector (1/2, 0, 1/2) can be understood, as schematically indicated Fig. 7b, as those nesting a folded FS (the folding is due to the doubling of the unit cell in the transverse intralayer direction. In addition the complete opening of the FS, required for a good nesting, needs probably the help of a secondary structural distortion which strong coupling with the primary distortion could explain the unusual 1st order nature of the CDW transition of this salt [80]). The 3rd component simply leads to an out phase ordering of layers of CDW, a configuration which minimizes the interlayer Coulomb interaction . Two different CDW ground states are stabilized below 150 K and 105 K in TTF $[Pd(dmit)_2]_2$ [41]. As shown Fig. 6, their CDW component in chain direction corresponds to the $2k_F$ nesting wave vectors of the bunch of quasi 1D bands derived from the LUMO and HOMO. The true reasons for the stabilization of either a SDW or a CDW ground states in these systems are not completely clear. It has been suggested [31] that the SDW ground state is favored by the presence of Unklapp electron-electron interactions in the 2 : 1 salts, where $4k_F$ amounts to an in chain reciprocal lattice wave vector (see ref. 4 for a critical review of the literature on this aspect).

In the strong coupling case, first a $4k_F$ Mott-Hubbard charge localization occurs in temperature (at about $T\rho \sim 200$ K at P_{atm} in the $(TMTTF)_2X$ series). When the charge degrees of freedom are frozen, two kinds of electronic ground states, involving the spin degrees of freedom are observed (Fig. 8) :

a) antiferromagnetic (AF) order of the spins : case of $(TMTTF)_2Br$ (T_N = 13 K) and $(t\text{-}TTF)_2Br$ (T_N = 33 K).

b) pairing of the spins in a singlet (S = 0) non-magnetic ground state via a lattice distortion (spin-Peierls (SP) transition) : case of $(TMTTF)_2PF_6$ (T_{sp} = 15-19 K) and $(BCP\text{-}TTF)_2PF_6$ (T_{sp} = 36 K).

Physical parameters controlling the stabilization of either the AF or the SP ground states in these quasi-1D systems are discussed in ref. 42.

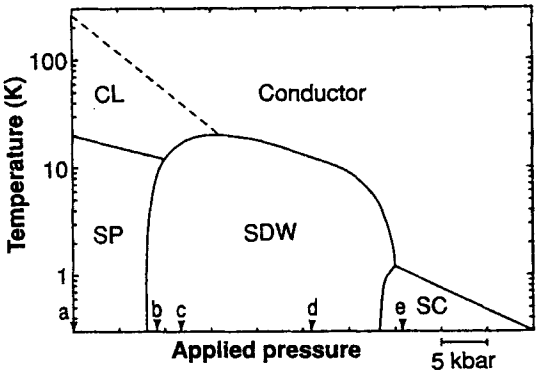

Figure 9
Generalized phase diagram for the (TMTTF-TMTSF)$_2$X series.
The notations SP, SDW and SC refer to spin-Peierls, spin density wave, and superconducting ground states, respectively. The dotted line marks the limit between conducting and charge-localized (CL) behavior. The letters designate compounds and indicate their location at atmospheric pressure in the generalized diagram: a : $(TMTTF)_2PF_6$, b :$(TMDTDSF)_2PF_6$, c : $(TMTTF)_2Br$, d : $(TMTSF)_2PF_6$ and e : $(TMTSF)_2ClO_4$ (from ref. 3a).

Some members of the (TMTTF-TMTSF)$_2$X series show an interesting generalized phase diagram [3a] (Fig. 9), where successively as a function of the pressure and of the member of the series : SP, SDW and superconducting ground states are stabilized. Two important parameters seem to control this phase diagram; from TMTTF to TMTSF and under pressure :

- the $4k_F$ electronic localization vanishes,
- the transverse interaction ($t_\perp$) increases.

The shape of the SDW phase is particularily interesting : T_{SDW} first increases, reaching a maximum when $T\rho$ vanishes, then decreases [43]. At first, in a 1D regime, the increase of T_{SDW} can be either due to the vanishing of the competing SP fluctuations or to the decrease of 1D fluctuations and increase of the interchain coupling (in a general manner 1D fluctuations depress the critical temperature, as there is no phase transition at finite temperature in a purely 1D system with finite range interactions). Then, in the quasi-1D regime the decrease of T_{SDW} could be related to the enhancement of the warping of the FS (increase of $t_\perp$) which deteriorates its nesting properties and thus the SDW instability. The same effect probably leads to the vanishing of the CDW insulating phase under pressure in

$(ET)_2 ReO_4$ and α-TTF $[Pd(dmit)_2]_2$. At the critical pressure at which the SDW or the CDW phases are suppressed, a maximum value of the superconducting critical temperature is observed. Such a behavior is not restricted to organic conductors. It is observed for example in the CDW inorganic quasi-1D conductor $NbSe_3$ [44].

Among the members of others families of quasi 1D conductors, $(DMET)_2 Au(CN)_2$ exhibits a phase diagram resembling that of $(TMTSF)_2PF_6$ with a competition under pressure between a SDW and a superconducting ground states [45].

Table III gives some measured valuesof the SDW and CDW gaps 2Δ. It is interesting to remark that the ratio $2\Delta/k_B T_c$, where T_c is the density wave ordering critical temperature, is greater for CDW than for SDW. In both cases the weak coupling BCS value of 3.5 is overcame.

The FS of 2D organic superconductors generally does not exhibit good nesting properties favoring a CDW or a SDW ground state. As a consequence superconductivity is generally observed at ambiant pressure in these salts.

V. ORDER-DISORDER TRANSITIONS OF STRUCTURAL DEGREES OF FREEDOM

Orientational and conformational degrees of freedom have a key control on the phase diagram of the organic conductors especially when disordered at ambiant temperature these degrees of freedom order upon cooling.

Let us first begin with the influence of the orientational order of the anions X. We have up now considered the $(TMTSF)_2X$ salts where X is, like PF_6, a centrosymmetrical anion. Bechgaard salts can also incorporate non centrosymmetrical anions like the tetrahedra ReO_4, ClO_4. Placed on an inversion center of the structure, these anions are disordered at room temperature. For entropy reasons they order collectively upon cooling at a T_{AO} ranging from 180 K (ReO_4) to 24 K (ClO_4). At ambiant pressure the ReO_4 adopt an alternate order in the stacking direction accompanied by a $2k_F$ CDW distortion of the TMTSF stack [46]. Because of the $2k_F$ periodicity a Peierls gap is opened, leading to a dielectric insulating ground state. The detailed mechanism of the anion ordering (AO) transition is not known. However, because of the large value of the gap 2Δ, comparable to t_a (~E_F in these 1/4 filled band systems) , and which is more than an order of magnitude greater than $k_B T_{AO}$ (see table III), a strong coupling theory is certainly required to describe the AO phase transition. Above about 10 Kbar the more natural uniform order between ReO_4 is observed in the stack direction [47] and the metallic state is recovered. Upon cooling $(TMTSF)_2ReO_4$ becomes a superconductor. Because of the freezing of the kinetics of

	Ground state	2Δ	$2\Delta/k_BT_c$	method
$(TMTSF)_2X$				
$R\text{-}ClO_4$	Supra	0.44 meV	4.2	tunneling
$Q\text{-}ClO_4$	SDW	1.9 meV	3.6	resistivity
PF_6	SDW	6 ± 1.3 meV	6 ± 1.3	IR reflectivity
ReO_4	A.O.	0.2 eV 0.17 eV	13 11	IR reflectivity conductivity
BF_4	A.O.	0.13 eV 0.17 eV	42 51	IR reflectivity conductivity
$(BEDTTTF)_2X$				
ReO_4	CDW	86 meV	13	resistivity
$\beta\text{-}AuI_2$	Supra	1.4 eV 5eV	4 15	tunneling point contact
$\kappa\text{-}Cu(NCS)_2$	Supra	4.8 ± 1.1 meV	5.1 ± 1.2	S.T.M.
$\kappa\text{-}Cu[N(CN)_2]Cl$	?	0.1 eV	23	IR reflectivity
$Y[Pd(dmit)_2]_2$				
C_S	CDW	40 meV	8.2	resistivity
TTF	CDW	0.13 eV	12 ± 2	resistivity

Table III

Ground state, energy gap, $2\Delta/k_BT_c$ ratio (BCS value = 3.5) and method of measurement of 2Δ in some quasi-1D and 2D organic conductors.

the AO at low temperature this uniform order can be kept by depressurization, revealing another insulating ground state (probably of SDW origin) which competes with the superconductivity [48].

The subtle interplay between SDW and superconductor ground states via the AO transition is also shown as a function of the cooling rate in $(TMTSF)_2ClO_4$ [4]. At low cooling rate (relaxed, R, samples) the ClO_4 anions order and the R salt becomes a supraconductor. At high cooling rate (quenched, Q, samples) most of the ClO_4 does not order for kinetic reasons [48]. The Q salt thus undergo a SDW non-metal transition at about 6 K. These different ground states are believed to be due to small modifications of the FS (and of its nesting properties) associated with lattice deformations accompanying the AO transition.

Conformational degrees of freedom of the ET molecules have also a subtle influence on the physical properties of $(ET)_2X$ salts.They concern the ethylene,C_2H_4, terminal groups of the ET which are at the basis of an hydrogen bond network linking ET and X species [50]. These two terminal groups can adopt either an eclipsed (E) or a staggered (S) configuration (Fig. 10). In most of the ET salts one out of two ethylene groups is disordered at room temperature. In the β phase it orders either in the E configuration at low temperature (X = I Br_2, AuI_2) or in the S configuration under modest pressure and low temperature (X = I_3). At ambiant pressure an incommensurate modulation of the occupancy of the S and E positions is observed [51] below 175 K in $(ET)_2 I_3$.This forms the so-called β_L state which has a T_S of 1.5 K, five times smaller than the T_S observed in the uniformly ordered "high pressure" β_H state. The origine of this incommensurate modulation, which involves also rigid displacements of I_3 and ET species, is not clearly established. Here we want to point out that if the driving mechanism is probably due to the ordering of the ethylene groups, the intralayer wave vector component $\vec{b}^* - \vec{Q}_{inc} = -0.08\,\vec{a}^* + 0.73\,\vec{b}^*$ of the ordering wave could be stabilizing in such a way to nest small portions of the FS shown Fig. 5b. In agreement with this possible mechanism, anomalies of $d\rho/dT$ and of the Hall constant are observed at 175 K. This nesting, and perhaps the opening of the FS along ΓC below 22 K [79], could lead to the formation of pockets of carriers around the X point, which are perhaps the clue to understand the huge reduction of T_S in the β_L phase. A detailed analysis of the pressure-temperature structural phase diagram has shown that the incommensurate modulated phase is metastable at ambiant pressure below about 125 K [52]. Thus the β_H uniformly (S) ordered ground state can be stabilized at ambiant pressure either by a low temperature depressurization process [53] or by waiting the thermodynamical transformation several

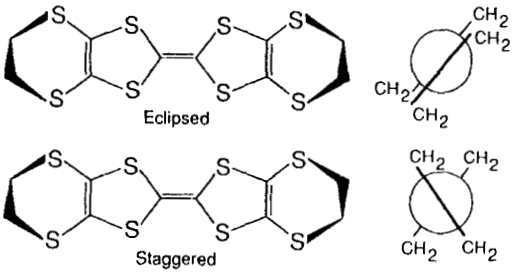

Figure 10
Eclipsed and staggered configurations of the ethylene group arrangement of the ET molecule.

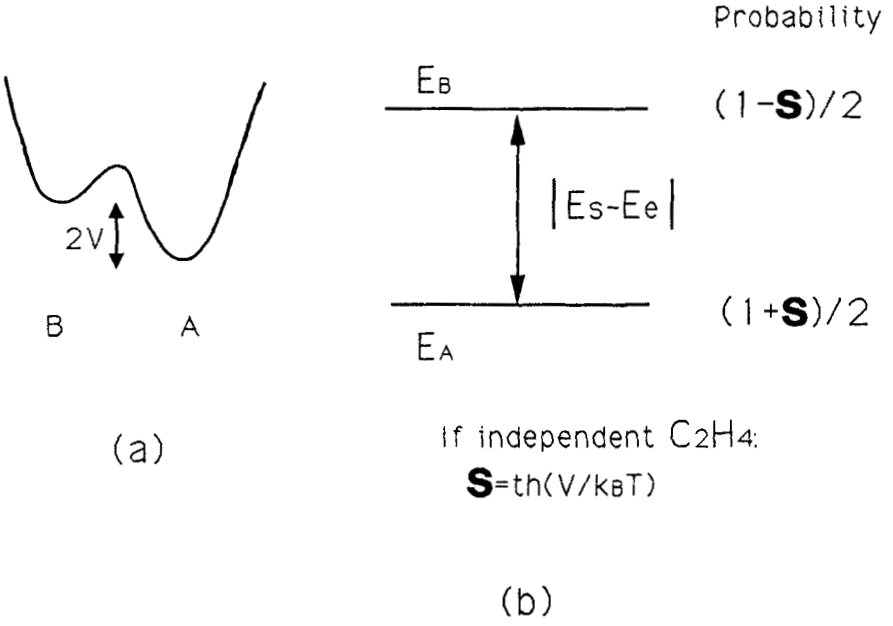

Figure 11
a) Schematic shape of the local potential seen by an ethylene group of the ET molecule. Occupancy of the wells A or B gives rise to the two stable (E or S) configurations of the molecule.
b) HOMO levels of the ET molecule for the A and B configurations with their probability of occupation. The expression of **S** given assumes non interaction between the C_2H_4 groups (the case of interacting C_2H_4 groups is considered in ref. 52).

days at about 110 K [54]. The β_H state can be locally induced below 125 K by irradiation defects which destroy the incommensurate modulation [55].

In relationship with this interpretation, it has also been suggested that the nesting of open quasi-1D portions of the FS of κ-$(ET)_2Cu(NCS)_2$ could help to stabilize a periodic succession of faults in the zig-zag sequence of the $Cu(NCS)_2$ polymeric chains [56].

Another intriguing feature which could be related to the ordering of C_2H_4 groups concerns the crossover from semiconductor to metallic behavior observed, at $T_{\rho max}$, in many ET salts adopting the κ structure. The link of this crossover with the C_2H_4 ordering is demonstrated by table IV showing that $T_{\rho max}$ is only observed in salts exhibiting a C_2H_4 disorder at room temperature. By analogy with the observation in the β phase, that the local potential seen by the C_2H_4 groups (fig. 11a) is very sensitive to the local environment, the amplitude and position of the maximum of resistivity are :

- enhanced and shifted towards lower temperatures under b-axis elongation [57].
- reduced and shifted towards higher temperatures under modest pressure [58].

The ordering of the C_2H_4 group certainly induces some changes in the H bonding network of the structure, which are probably responsible of the anomalous thermal dependence shown by some lattice parameters around $T_{\rho max}$ [59]. The disorder of the ethylene groups could lead at high temperature to an Anderson localization of the carriers especially if the difference of energy between the HOMO levels corresponding to the S and E molecular configurations, $|E_S-E_E|$ in Fig. 11b, is comparable to the intermolecular transfer integrals ($t_{intradimer} \sim 0.25$ eV and $t_{interdimer} \sim 0.1$ eV). The $|E_S-E_E|$ splitting is probably due to ET molecular deformations depending upon the ethylene group arrangement. The occupancy of the highest energy molecular level being suppressed at low temperature (i.e. when $k_BT < V$ in the case of no interaction between neighbouring C_2H_4 groups) by the stabilization of a S or E ground state configuration of the ET molecule, the metallic behavior is recovered and superconductivity is generally observed around 10 K.

A similar crossover from a semiconducting to a metallic (and superconducting) state is observed in $(CH_3)_4$ N $[Pd(dmit)_2]_2$ under pressure [60]. The low pressure semiconducting behavior is probably caused by an electron localization due to the orientational disorder of the $(CH_3)_4N$ cations.

	T_s	$T_{\rho max}$	C_2H_4 order	
			R.T.	at low temperature
$(ET)_2 I_3$	3.6 K	No	Yes (E)	
$(ET)_2Cu(NCS)_2$	10.4 K	Yes (~90 K)+	No	Yes (S)
$(ET)_2Cu\ N(CN)_2Br$	11.6 K	Yes (~100 K)	No	Yes (E)
$(ET)_2Cu\ N(CN)_2Cl$	No T_s [metal-insulator] transition at ~ 50K]		No	Yes (E)
$(ET)_2Cu\ N(CN)_2I$	No T_s[electron localization below 150 K]		No	incomplete (E/S = 2/1)
$(ET)_2Cu\ N(CN)_2CN$	~ 11 K	No	Yes (S and E)	
$(ET)_2Cu_2\ (CN)_3$	No T_s	Yes (~ 20 K)+	No	Yes
	2-3.8 K	No	Yes (S)	
+ sample dependent				

Table IV

Critical temperature of superconductivity (T_s), temperature of semiconductor to metal crossover deduced from the temperature of maximum resistivity ($T_{\rho max}$), and ethylene order of the ET molecule at ambiant pressure for some $(ET)_2X$ salts adopting the κ structure. E (eclipsed) and S (staggered) correspond to the two relative configurations of the two terminal C_2H_4 groups of the ET molecule shown figure 10. No in the $T_{\rho max}$ column means metallic behavior below room temperature.

VI THE SUPERCONDUCTOR GROUND STATE

Organic superconductors exhibit many common features. In quasi-1D salts a maximum value of T_S is achieved at the boarderline of a competing SDW [$(TMTSF)_2X$] or CDW [TTF [$Pd(dmit)_2]_2$] ground state. All the 1D or 2D organic superconductors show a decrease of T_s under pressure with a rate :

$$\frac{\partial \ln T_S}{\partial P} \sim -[0.1\text{-}0.3]\ (\text{Kbar})^{-1}$$

The same rate of decrease is observed in K_3C_{60} and RbC_{60} [-(0.3-0.4) $Kbar^{-1}$] [61], and even in $NbSe_3$ [$-0.2(Kbar)^{-1}$] [44]. In fullerene materials it is observed a correlation between the increase T_S and the increase of lattice parameter [62]. In a similar way it has been proposed a correlation between T_S and either the effective volume per ET molecule [63] or the anion length in $\beta(ET)_2X$ [64].

Figure 12 gives that the Ginzburg Landau coherence length measured in the superconducting state (for a proper determination of this quantity see ref. 65) in the 1D direction and the 2D layer of $(TMTSF)_2X$ and $(ET)_2X$ salts respectively. These $\xi_{//}$ as well as ξ measured in superconducting fullerenes follow roughly the same $\xi \sim T_S^{-1}$ dependence expected in the case of pure (or clean) superconductors where :

$$\xi \sim \xi_0 = \frac{h v_F}{\pi \Delta_s}, \quad \text{with } \Delta_s \alpha T_S \qquad (4)$$

(Additional evidences for a clean limit come from magnetic penetration depth measurements [66]). According to the expression (4) ξ decreases with the increase of the strength of the pairing interaction, Δ_s, a quantity related to T_S. In particular ξ is less than ~ 100 Å in $\kappa(ET)_2$ X and between 20-30 Å in the fullerenes. Figure 12, reporting also the interlayer coherence lengths, shows that in the low T_S salts $\xi_\perp$ is a slightly greater than the interlayer spacing and that in the high T_S salts $\xi_\perp$ is smaller than the interlayer spacing. This places these materials at the boarderline between 3D anisotropic and 2D superconductors.

A third feature is that all these organic materials are type II superconductors with a magnetic field London penetration depth λ larger than ξ ; in $\beta(ET)_2AuI_2$: $\lambda_{//} \sim 4\ 10^4$Å and $\lambda_\perp \sim 5\ 10^3$ Å , while in κ-$(ET)_2X$: $\lambda_\perp \sim (9.8 - 7.8)\ 10^3$Å , to be compared with $\lambda \sim (2.5 - 4.5)\ 10^3$Å in the fullerenes . In the κ phases it is also found from λ measurements [66] that Eq(5), with a SdH carrier mass of $m^* \sim 3.5\ m_e$, gives a superconducting carrier density n_s which amounts to about that included in the hole pockets of the FS (see fig. 5c).

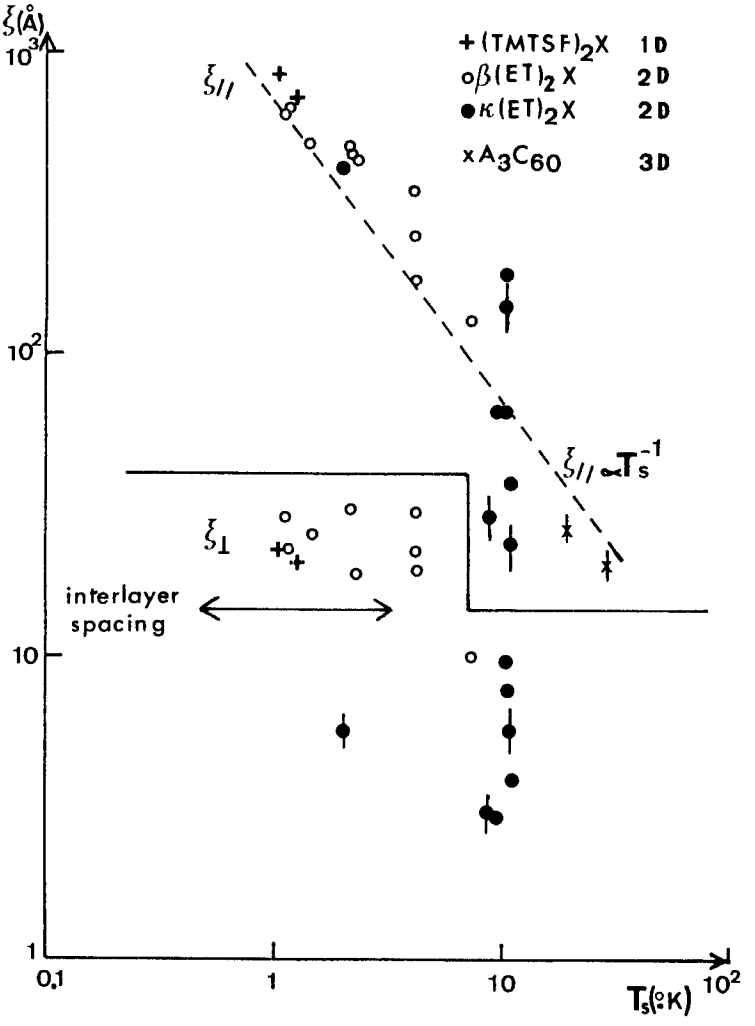

Figure 12

Coherence lengths in the 1D direction or the 2D conducting plane ($\xi_{//}$) and in the interlayer direction ($\xi_{\perp}$) in function of T_S for various organic superconductors. For comparison ξ determined in the 3D fullerene superconductors is also indicated.

At this level it is worth mentioning that basic similarities exist between ($\kappa(ET)_2X$, Y_3C_{60}) organics and cuprates, bismuthate, Chevrel phases, heavy Fermion superconductors. All these materials are extreme type II superconductors with a short ξ and a large λ. Penetration depth measurements [72] show that these exotic superconductors are characterized by a low n_s/m^* value, according to the relationship

$$\frac{c^2}{\lambda^2} = \frac{4\pi n_s e^2}{m^*}, \qquad (5)$$

valid in the clean limit. Small n_s/m^* means a Fermi energy only two order of magnitude greater than T_S and comparable to the energy of the boson mediating the superconducting pairing [78]. This last feature questions the effectiveness of retardation effects which are at the basis of the conventional theory of superconductivity. In addition the finding of a short ξ means the presence of local bosons with an average interpair separation not negligeable with respect to the thermal wave length of the pair, corresponding to a situation close to that required for a Bose Einstein condensation [72] (such a condensation occurs when these two last lengths are comparable). These experimental findings encourage the development of a new theory of superconductivity, with low carrier densities and strong pairing interactions, which interpolates between the BCS theory and the Bose-Einstein condensation.

Finally let us point out that these exotic superconductors exhibit also non conventional electronic structures. They are either 2D conductors (organics, cuprates) or constituted of weakly coupled units (inorganic clusters in Chevrel phases, C_{60} molecules in the fullerenes, dimers in the $\kappa(ET)_2X$ organics). The influence of these different scales of electronic energy on the critical temperature of superconductivity remains to be fully understood [81].

Important questions also concern the superconducting pairing mechanism in these organic materials :

a) what are the excitations (bosons) leading to an attractive interaction between electrons ?

b) what is the strength of the coupling ($2\Delta_S/k_BT_S$ ratio) ?

c) what is the symmetry of the pairing (of Cooper pair wave functions) ?

In principle tunneling experiments can answer question b. Most of the experiments give $2\Delta_S/k_BT \sim 4\text{-}5$ (Table III), which is slightly above the BCS weak coupling value of 3.5. A somewhat larger ratio of 5.3 is found in Rb_3C_{60} [67]. It is

also claimed that from the theoretical evaluation of the coherence length of organic superconductors, the ordinary BCS formulae describe the situation quite well in the vicinity of T_c [68].

The experimental situation concerning the symmetry of the pairing (question c) is not so clear . Muon-spin lattice relaxation measurements of the very low temperature dependence of the magnetic penetration depth, $\lambda(T)$, in $\kappa(ET)_2X$ with X = $Cu(NCS)_2$ and $Cu[N(CN)_2]Br$ are consistent with an anisotropic superconducting pairing with line rods in the energy gap [66]. On the other hand the observation in the former salt of a coherence peak from microwave impedance measurements has been taken as a signature of conventional s-wave isotropic coupling [69]. The absence of a T_1 coherence peak in $(TMTSF)_2ClO_4$ suggests a non isotropic pairing [70]. In fullerene materials muon-spin relaxation measurements of $\lambda(T)$ suggest a singlet s-wave pairing [71].

The study of new types of pairing mechanism in organic materials really started in 1964 with the proposal of Little [73] that intramolecular electronic excitations could play the role of the phonons in the ordinary superconductors. Up to now there is no evidence for such a mechanism in organic superconductors. Two kinds of mechanisms have been proposed (for a critical review see [4]). In $(TMTSF)_2X$ materials, where the SDW and superconducting phases are neighbors it has been suggested that an attractive interaction between carriers belonging to neighbouring chains can be mediated by spin fluctuations [74]. In the $(ET)_2X$ salts more conventional mechanisms involving phonons, have been considered. There has been several evaluations of T_S in the framework of the BCS theory of superconductivity by considering either low frequency phonons associated with the translational or librational modes of vibration (and whose softening is strongly influenced by the C-H-donor and C-H-anion contacts) [75] or with the particularly strong intramolecular EMV coupling of the TTF based molecule [4]. Both positive and negative isotope effects have been reported on the T_S of $(ET)_2X$ superconductors, which up to now does not give a real insight concerning the pertinent phonon modes. Finally it would be very surprising if a common mechanism could not exist in all these TTF based organic materials.

A large number of mechanismshas been proposed to explain superconductivity of fullerenes, which T_S is about 2 orders of magnitude larger than the T_S of graphite intercalation compounds. Among them a special attention has been devoted to the electron-phonon coupling which could be especially strong in the fullerenes because of the spherical shape of the C_{60} molecule [77] or because of the ionic fcc lattice

structure[76]. In agreement with the electron-phonon coupling mechanisms a positive isotope effect is observed. However there is up to now no experimental agreement on the magnitude of this effect.

Acknowledgements

The author is very greatfull to E. Canadell, D. Jérome, R. Moret and S. Ravy for numerous discussions on the organic conductors and to K. Holczer for a discussion on the fullerenes.

REFERENCES

1. Physical properties of charge transfer salts are reviewed in :
- D. Jérome and H.J. Schulz, Adv. Phys. 31, 299 (1982)
- E.M. Conwell (Editor) "Highly Conducting Quasi One Dimensional Organic Crystals" - Semiconductors and Semimetal Vol 27 (Academic Press 1988)
2. D. Jérome, A. Mazaud, M. Ribault and K. Bechgaard, J. Physique Lettres 41, L 95 (1980)
3. For short recent reviews see
a) D. Jérome, Science 252, 1509 (1991)
b) J.M. Williams, A.J. Schultz, U. Geiser, K.D. Carlson, A.M. Kini, H.H. Wang, W.K. Kwok, M.H. Whangbo and J.E. Schirber, Science, 252, 1501 (1991)
c) K. Prassides and K. Kroto, Physics World 5, 44 (1992)
4. For a recent book see :
T. Ishiguro and K. Yamaji "Organic Superconductors" - Springer Series in Solid State Sciences, Vol 88 (Springer Verlag, Berlin, Heidelberg 1990)
5. J.P. Pouget, S. Ravy and R. Moret, Phase transitions 14, 261 (1989)
6. S. Ravy, E. Canadell, J.P. Pouget, P. Cassoux, A.E. Underhill, Synth. Metals 41-43, 2191 (1991) and earlier references therein
7. S. Saito and A. Oshiyama, Phys. Rev. Lett. 66, 2637 (1991)
8 T. Granier, B. Gallois, L. Ducasse, A. Fritsch and A. Filhol, Synth. Metals 24, 343 (1988)
9 (a) P.M. Grant, J. Physique Colloque 44, C3 - 847 (1983)
(b) L. Ducasse, M. Abderrabba, J. Hoarau, M. Pesquer, B. Gallois and J. Gaultier, J. Phys. C 19, 3805 (1986)
(c) B. Gallois, J. Gaultier, T. Lamcharfi, F. Bechtel, A. filhol, L. Ducasse and M. Abderrabba, Synth. Metals 19, 321 (1987)
10. a) T. Mori, A. Kobayashi, Y. Sasaki, H. Kobayashi, G. Saito, H. Inokuchi, Chem. Lett. 957 (1984)
b) M.H. Whangbo, P.C.W. Leung, M.A. Beno, T.J. Enge, H. H.Wang, K.D.Carlson and G.W. Crabtree, J.A.C.S. 107, 5815 (1983)
c) T. Mori and H. Inokuchi, J. Phys. Soc. Japan 57, 3674 (1988)
11. M.H. Whangbo, M.A. Beno, P.C.W. Leung, T.J. Emge, H.H. Wang and J.M. Williams Solid State Commun 59, 813 (1986)
12. a) D. Jung, M. Evain, J.J. Novoa, M.H. Whangbo, M.A. Beno, A.M. Kini, A.J. Schultz, J.M. Williams and P.J. Nigrey, Inorganic Chem 28, 4516 (1989)
b) P. Delhaes, J. Amiell, S. Flandrois, L. Ducasse, A. Fritsch, B. Hilti, C.W. Mayer, J. Zambounis and G.C. Papavissiliou, J. Phys.France 51, 1179 (1990)

13. L. Ducasse and A. Fritsch, Synth. Metals 27, B 1 (1988)
14. C.S. Jacobsen, D.B. Tanner and K. Bechgaard, Phys. Rev. Lett. 46, 1142 (1981)
15. W. Kang, G. Montambaux, J.R. Cooper, D. Jérome, P. Batail and C. Lenoir, Phys. Rev. Lett. 62, 2559 (1989)
16. M.V. Kartsovnik, V.N. Laukhin, S.I. Pesotskii, I.F. Schegolev and V.M. Yakovenko, J. Physique 2, 89 (1992)
17. a) C.S. Jacobsen, J.M. Williams and H.H. Wang, Solid State Commun. 54, 937 (1985) [Erratum 57, i (1986)]
    b) M. Kuroda, K. Yakushi, H. Tajima, A.Ugawa, Y. Okawa, A. Kobayashi, R. Kato, H. Kobayashi and G. Saito, Synth. Metals 27, A 491 (1988)
18. K. Oshima, T. Mori, H. Inokuchi, H. Urayama, H. Yamochi and G. Saito, Phys. Rev. B 38, 938 (1988)
19. R.C. Yu, J.M. Williams, H.H. Wang, J.E. Thompson, A.M. Kini, K.D. Carlson, J. Ren, M.H. Whangbo and P.M. Chaikin, Phys. Rev. B 44, 6932 (1991)
20. T. Osada, A. Kawasumi, S. Kagoshima, N. Miura and G. Saito, Phys. Rev. Lett. 66, 1525 (1991)
21. See for example the contributions of K.Yamaji, K. Kajita et al and T. Osada et al in part V of "The Physics and Chemistry of Organic superconductors" Springer Proceedings in Physics 51, Edited by G. Saito and S. Kagoshima (Springer Verlag Berlin 1990)
22. J. Wosnitza, G.W. Crabtree, H.H. Wang, U. Geiser, J.M. Williams and K.D. Carlson, Phys. Rev. B 45, 3018 (1992) and Phys. Rev. Lett. 67, 263 (1991)
23. E. Canadell, I.E. - I Rachidi, S. Ravy, J.P. Pouget, L. Brossard, J.P. Legros, J. Physique 50, 2967 (1989)
24. Y. Maruyama, this conference
25. J.B. Torrance, B.A. Scott, F.B. Kaufman,, Solid State Commun. 17, 1369 (1973)
    C.S. Jacobsen, I.Johannsen and K. Bechgaard, Phys. Rev. Lett. 53, 194 (1984)
26. G. Soda, D. Jérome, M. Weger, J. Alizon, J. Gallice, H. Robert, J.M. Fabre and L. Giral, J. Physique 38, 931 (1977)
    T. Takahashi, D. Jérome, F. Masin, J.M. Fabre and L. Giral, J. Phys. C : Solid State 17, 3777 (1984)
27. J.P. Pouget, S.K. Khanna, F. Dénoyer, R.Comès, A.F. Garito and A.J.Heeger, Phys. Rev. Lett. 37, 437 (1976)
    A.J. Epstein, J.S. Miller, J.P. Pouget and R. Comès, Phys. Rev. Lett. 47, 741 (1981)
28. C. Bourbonnais, P. Wzietek, F. Creuzet, D. Jérome, P. Batail and K. Bechgaard, Phys. Rev. Lett. 62, 1532 (1989) and J. Physique (to be published).
29. C.S. Jacobsen, J. Phys. C : Solid State Physique 19, 5643 (1986)
30. a) C. Coulon, P. Dehaes, S. Flandrois, R. Lagnier, E. Bonjour and J.M. Fabre, J. Physique 43, 1059 (1982)
    b) R. Laversanne, C. Coulon, B. Gallois, J.P. Pouget and R. Moret, J. Physique Lett. 45, L393 (1984)
31. V.J. Emery, R. Bruinsma and S. Barisic, Phys. Rev. Lett. 48 1039 (1982)
32. C. Coulon in "Organic and Inorganic Low Dimensional Crystalline Materials" Edited by P. Delhaes and M. Drillon, NATO ASI Series B 168 (Plenum Press, New York 1987), p 201
33 P.M. Allemand, K.C. Khemani, A. Koch, F. Wudl, K. Holczer, S. Donovan, G. Gruner and J.D. Thomas, Science 253, 301 (1991)

34. S. Ravy, J.P. Pouget and B. Hennion Phase transition 30, 5 (1991)
35. M. Krauzman, J. Breitenstein and R.M. Pick in "Laser Optics of Condensed Matter " Vol 2 Ed. by A. Maradudin, E. Garmire and K.K. Rebane (Plenum Press -New York)
36. N. Toyota and T. Sasaki, Solid. State Commun 74, 361 (1990)
37. C.S. Cariss, L.C. Porter and R.J. Thorn, Solid State Commun. 74, 1269 (1990)
38. J. Singleton, F.L. Pratt, M. Doporto, T.J.B.M. Janssen, M. Kurmoo, J.A.A.J. Perenboom, W. Hayes and P. Day, Phys. Rev. Lett 66, 2500 (1992)
39. J.M. Delrieu, M. Roger, Z. Toffano, A. Moradpour and K. Bechgaard, J. Physique 47, 839 (1986)
T. Takahashi, Y. Maniwa, H. Kawamura and G. Saito, J. Phys. Soc. Japan 55, 1364 (1986)
40. S. Ravy, R. Moret, J.P. Pouget, R. Comès and S.S.P. Parkin, Phys. Rev. B 33, 2048 (1986)
41. S. Ravy, J.P. Pouget, L. Valade, J.P. Legros, Europhys. Lett. 9, 391 (1989)
42. P. Vaca and C.Coulon, Phase Transitions 30, 49 (1991)
43. P. Auban, D. Jérome, K. Lerstrup, I. Johannsen, M. Jorgensen and K.Bechgaard, J. Phys. France 50, 2727 (1989)
44. N. Nunez Regueiro, J.M. Mignot and D. Castello, Europhys. Lett. 18, 53 (1992)
45. Y. Honda, K. Murata, K. Kikuchi, K. Saito, I. Ikemoto and K. Kobayashi, Solid State Commun 71, 1087 (1989)
46. R. Moret, J.P. Pouget, R. Comès and K. Bechgaard, Phys. Rev. Lett. 49, 1008 (1982)
47. R. Moret, S. Ravy, J.P. Pouget, R. Comès and K. Bechgaard, Phys. Rev. Lett.57, 1915 (1986)
48. S. Tomic and D. Jérome, J. Phys. Cond. Matter. 1, 4451 (1989)
49. J.P. Pouget, S. Kagoshima, T. Tamegai, Y. Nogami, K. Kubo, T. Nakajima and K. Bechgaard, J. Phys. Soc. Japan 59, 2036 (1990)
50. M.H. Whangbo, D. Jung, J. Ren, M. Evain, J.J. Novoa, F. Mota, S. Alvarez, J.M. Williams, M.A. Beno, A.M. Kini, H.H. Wang and J.R. Ferraro in ref. 21 p 262
51. P.C.W. Leung, T.J. Enge, M.A. Beno, H.H. Wang, J.M. Williams, V. Petricek and P. Coppens, J. Am. Chem. Soc. 107, 6184 (1985)
52. S. Ravy, R. Moret and J.P. Pouget, Phys. Rev. B 38, 4469 (1988)
53. F. Creuzet, G. Creuzet, D. Jérome, D. Schweitzer and M.J.Keller, J. Phys. Lett. 46, L 1079 (1985)
54 See the contributions of S. Kagoshima et al., Y. Nogami et al, K. Kanoda et al, M. Tokumoto et al., T. Sasaki et al. in part IV of ref. 21
55. S. Ravy, J.P. Pouget, R. Moret and C. Lenoir, Phys. Rev. B 37, 5113 (1980)
56. S. Ravy, J.P. Pouget, C. Lenoir and P. Batail, Solid State Commun. 73, 37 (1990). The ET layer is composed of orthogonal dimers let say situated in (0,0) and (1/2, z) in the (b,c) sheet. The more likely effect of the cis to trans conformational defects of the polymeric chain is to displace the z coordinate of the 2nd dimer to 1-z. This interchanges the inequivalent up and down hydrogen bonding between the ET and the two neighbouring $Cu(NCS)_2$ in the interlayer a direction (S. Ravy, private communication)
57. M. Kusuhara, T. Sakata, Y. Ueba, K. Tada, M. Kaji and T. Ishiguro, Solid State Commun. 74, 251 (1990)

58. K. Murata, Y. Konda, H. Anzai, M. Tokumoto, K. Takahashi, N. Kinoshita, T. Ishiguro, Synth. Metals 27, A 263 (1989)
W. Kang, D. Jérome, C. Lenoir and P. Batail, J. Phys. Condens. Matter, 2, 1665 (1990)
J.E. Schirber, D.L. Overmyer, K.D. Carlson, J.M. Williams, A.M. Kini, H.H. Wang, H.A. Charlier, B.J. Love, D.M. Watkins and G.A. Yaconi, Phys. Rev.B 44, 4666 (1991)
Y.V. Sushko, V.A. Bondarenko, R.A. Petrosov, N.D. Kushch and E.B. Yagubskii, J. Physique 1, 1375 (1991)
59. Y. Watanabe, T. Sasaki, H. Sato and N. Toyota, J. Phys. Soc. Japan 60, 2118 and 3608 (1991)
K. Andres, C.P. Heidmann, H. Muller, S. Himmelsbach, W.Biberacher, C.H.Probst and W. Joss, Synth. Metals 41-43, 1983 (1991)
60. A. Kobayashi, H. Kobayashi, A. Miyamoto, R. Kato, R.A. Clark and A.E. Underhill, Chem. Letters p. 2163 (1991)
61. G. Sparn, J.D. Thompson, R.L. Whetten, S.M. Huang, R.B. Kaner, F. Diederich, G. Gruner and K. Holczer, Phys. Rev. Lett. 68, 1228 (1992)
62. R.M. Fleming, D.P. Ramirez, M.J. Rosseinsky, D.W. Murphy, R.C. Haddon, S.M. Zahurak and A.V. Makhija, Nature 352, 787 (1991)
63. G. Saito, T. Komatsu, T. Nakamura and H. Yamochi, Mat. Res. Soc. Symp. (Boston Dec. 1991) (under press)
64. J.M. Williams et al in "Lower-Dimensional Systems and Molecular Electronics" NATO ASI B248, Edited by R.M. Metzger, P. Day and G.C. Papavassiliou (Plenum Press New York 1991)
65. H. Ito, M. Watanabe, Y. Nogami, T. Ishiguro, T. Komatsu, G. Saito and N.Hosoito, J. Phys. Soc. Japan 60, 3230 (1991)
66. L.P. Le et al, Phys. Rev. Lett. 68, 1923 (1992)
67. Z. Zhang, C-C. Chen, S.P. Kelty, H. Dai and C.M. Lieber, Nature 353, 333 (1991)
68. I.F. Schegolev and E.B. Yagubskii, Physica C 185-189, 2433 (1991)
69. O. Klein , K. Holczer, G. Gruner, J.J. Chang and F. Wudl, Phys. Rev. lett. 66, 655 (1991)
70. M. Takigawa, H. Yasuoka and G. Saito, J. Phys. Soc. Japan 56, 873 (1987)
71. Y.J. Uemura et al, Nature 352, 605 (1991)
72. Y.J. Uemura et al. Phys. Rev. Lett. 66, 2665 (1991)
73. W.A. Little, Phys. Rev. 134, A 1416 (1964)
74. V.J. Emery, Synth. Metals 13, 21 (1986)
C. Bourbonnais and L.G. Garon, Europhys. Lett. 5, 209 (1988)
75. M.H. Whangbo, J.M. Williams, A.J. Schultz, T.J. Enge and M.A. Beno, J.A.C.S. 109, 90 (1987)
U. Geisser et al, Physica C 174, 475 (1991)
76. F.C. Zhang, M. Ogato and T.M. Rice, Phys. Rev. Lett. 67, 3452 (1991)
77. M.A. Schluter, M. Lannoo, M. Needels, G.A. Baraff and D. Tomanek, Phys. Rev. Lett. 68, 526 (1992)
78. L. Pietronero, Europhys. Lett. 17, 365 (1992)
79. N.A. Fortune, K. Murata, K. Ikeda and T. Takahashi, Phys. Rev. Lett. 68, 2933 (1992)
80. M.H. Whangbo, J. Ren, W. Liang, E. Canadell, J.P. Pouget, S. Ravy, J.M. Williams and M.A. Beno, to be published
81. J. Friedel, J. Phys. II (France) 2, 959 (1992)